Renewable and Sustainable Energy Reviews 110 (2019) 207–219

Contents lists available at ScienceDirect

Renewable and Sustainable Energy Reviews

journal homepage: www.elsevier.com/locate/rser

Gas switching reforming for flexible power and hydrogen production to balance variable renewables

Szabolcs Szima[a], Shareq Mohd Nazir[b], Schalk Cloete[c], Shahriar Amini[c,*], Szabolcs Fogarasi[a], Ana-Maria Cormos[a], Calin-Cristian Cormos[a]

[a] Faculty of Chemistry and Chemical Engineering, Babes - Bolyai University, Cluj – Napoca, Romania
[b] Department of Energy and Process Engineering, Norwegian University of Science and Technology, Trondheim, Norway
[c] Flow Technology Group, SINTEF Industry, Trondheim, Norway

ARTICLE INFO

Keywords:
CO_2 capture
Natural gas
Wind power
Solar power
Variable renewable energy
Gas switching reforming
Flexible power plant
Economic assessment

ABSTRACT

Variable renewable energy (VRE) is expected to play a major role in the decarbonization of the electricity sector. However, decarbonization via VRE requires a fleet of flexible dispatchable plants with low CO_2 emissions to supply clean power during times with limited wind and sunlight. These plants will need to operate at reduced capacity factors with frequent ramps in electricity output, posing techno-economic challenges. This study therefore presents an economic assessment of a new near-zero emission power plant designed for this purpose. The gas switching reforming combined cycle (GSR-CC) plant can produce electricity during times of low VRE output and hydrogen during times of high VRE output. This product flexibility allows the plant to operate continuously, even when high VRE output makes electricity production uneconomical. Although the CO_2 avoidance cost of the GSR-CC plant (€61/ton) was similar to the benchmark post-combustion CO_2 capture plant under baseload operation, GSR-CC clearly outperformed the benchmark in a more realistic scenario where continued VRE expansion forces power plants into mid-load operation (45% capacity factor). In this scenario, GSR-CC promises a 5 %-point higher annualized investment return than the post-combustion benchmark. GSR-CC therefore appears to be a promising concept for a future scenario with high VRE market share and CO_2 prices, provided that a large market for clean hydrogen is established.

1. Introduction

The recently released IPCC special report on global warming of 1.5 °C [1] has reemphasized the urgency of addressing anthropogenic climate change. Five main channels for greenhouse gas reduction are generally considered in global energy analyses (e.g. IEA [2]): energy efficiency, renewable energy, nuclear power, fuel switching, and CO_2 capture and storage (CCS).

Currently, solar photovoltaics (PV) is the only clean energy supply technology that is on track to meet the International Energy Agency's Sustainable Development Scenario (SDS) target [3], although wind power is also on track in several world regions. The SDS will result in global warming of 1.7–1.8 °C. CCS, which represents a group of technologies without which decarbonization efforts consistent with 1.5–2 °C will become much more expensive or even impossible [4], is far off track [3].

Given the success of solar PV and wind power, the electricity sector is expected to play a leading role in the decarbonization of the global energy sector. These variable renewable energy (VRE) technologies have shown impressive cost declines since the turn of the century [5], but they impose large integration challenges that will require a radical energy system transformation over coming decades.

1.1. Variable renewable energy (VRE) integration challenges

Hirth [6] identifies three major integration costs for VRE. The first and most important of these is profile costs. This cost is related to the temporal variability of wind and solar power, i.e. the fact that they only produce power when the wind blows or the sun shines. In practice, profile costs manifest as a value decline of wind and solar power. Fig. 1 illustrates this dynamic using recent real-world data from Germany and modelled VRE value declines resulting from an expansion of wind and solar power in Europe. As shown in Fig. 1 (left), the average unit of electricity from hard coal and gas plants is already worth 50% more than the average unit of electricity from wind in Germany.

Grid-related costs represent the second most important VRE

* Corresponding author.
E-mail address: shahriar.amini@sintef.no (S. Amini).

https://doi.org/10.1016/j.rser.2019.03.061
Received 15 January 2019; Received in revised form 19 March 2019; Accepted 30 March 2019
Available online 06 May 2019

List of abbreviations

ACF	annual cash flow
CA	CO_2 avoided
CC	combined cycle
CCR	CO_2 capture ratio
CCS	CO_2 capture and storage
COCA	cost of CO_2 avoidance
CEPCI	chemical engineering plant cost index
GSR	gas switching reforming
IEA	International Energy Agency
IPCC	Intergovernmental Panel on Climate Change
LCOE	levelized cost of electricity
LHV	lower heating value
MEA	monoethanolamine
NG	natural gas
NGCC	natural gas combined cycle
NPV	net present value
O&M	operating and maintenance
PSA	pressure swing adsorption
PV	photovoltaics
SDS	sustainable development scenario
SMR	steam methane reforming
ST	steam turbine
S/C	steam to carbon
TOC	total overnight cost
T&S	transport and storage
VRE	variable renewable energy
WGS	water-gas shift
η_{H2}	hydrogen production efficiency
$\eta_{H2,eq}$	equivalent hydrogen production efficiency

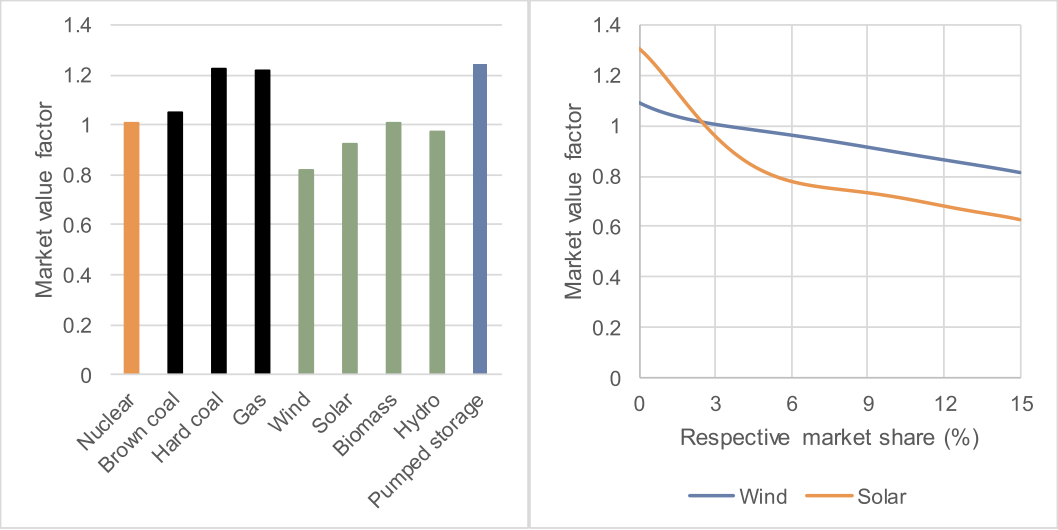

Fig. 1. Market value factors (volume-weighted market price for each technology divided by the time-averaged market price). Left: Data from Germany for the year 2017 [7]. Right: Simulated value decline of wind and solar power with increasing market share in Europe [8].

integration cost. These costs are related to the spatial variability of wind and solar resources, which require these generators to be concentrated in windy and sunny regions. The produced power must then be exported to demand centres via an expanded electricity transmission network. If the grid is not expanded at a sufficient rate, grid congestion occurs, forcing VRE curtailment and uneconomical operation of dispatchable generators (redispatch). As an example of these added costs, the Energiewende tracker from McKinsey and Co [9] currently measures the cost of network interventions at €9.9/MWh of wind and solar power, which amounts to fully 35% of the volume weighted market value of wind and solar power in 2017 [7].

The final integration cost component is referred to as balancing costs. This is generally the least important component and relates to the uncertainty in forecasting wind and solar output for planning electricity supply in day-ahead markets. Estimates of this cost vary widely, but the average spans from about €2/MWh at minor market shares to €4/MWh at 40% VRE market share [10].

Despite these challenges, multiple studies suggest the feasibility of 100% renewable energy systems, primarily based on wind and solar power (e.g. Jacobson and Delucchi [11]). However, these works have been countered by studies stating that a more balanced energy portfolio including nuclear and fossil fuels with or without CCS provides a more feasible pathway and that limiting the diversity of energy options can be counter-productive (e.g. Clack et al. [12]). Assessments from the IEA [2] and IPCC [4] continue to include a balanced technology portfolio in their decarbonization scenarios.

Another important factor that is often neglected is the economic challenges related to the expansion of capital-intensive wind and solar power in regions where the time-value of money (discount rate) is high. Hirth and Steckel [13] found that the cost-optimal share of renewables was 40% when the weighted average cost of capital (WACC) was only 3%, but this share fell to almost zero when the WACC increased to 15%. The WACC for energy technologies is generally around 7% in developed countries and 14% in developing countries [14]. Decarbonization with wind and solar in developing countries, where about 80% of new generating capacity will be constructed [2], will therefore be challenging.

Based on the factors thus far discussed, it can be reasonably assumed that the need for dispatchable thermal power plants will remain strong even as wind and solar power costs continue to decline and CO_2 prices gradually increase. Given that, by 2050, the global electricity sector must achieve net negative emissions in the 1.5 °C scenario and net-zero emissions in the 2 °C scenario [1], it is clear that these dispatchable thermal power plants will need to be decarbonized via CCS.

1.2. Flexible CO_2 capture

A comprehensive study by Brouwer et al. [15] found that natural

gas combined cycle (NGCC) plants equipped with CCS emerge as a low-cost option for balancing VRE, becoming especially useful for supplying seasonal flexibility. Other economic flexibility options included demand response (although the potential of this mechanism is limited and uncertain) and curtailment of excess VRE. Increased interconnection had only a marginal effect, whereas energy storage was uneconomical. The same authors studied the performance of thermal generators in a system with high shares of VRE [16], showing that thermal plants can provide sufficient flexibility in high VRE systems and that CCS must play a large role when low-carbon scenarios are considered.

CCS plants with post-combustion CO_2 capture can contribute further to flexibility by concentrating most of the energy penalty of CO_2 capture during times of low electricity demand. van der Wijk et al. [17] found that wholesale revenues from such measures only increase marginally, but that flexible CO_2 capture can lead to large increases in reserve provision. Increasing flexibility by venting CO_2 during times of high electricity demand is only profitable at moderate CO_2 prices.

Oates et al. [18] studied the profitability of flexible operation of coal and gas plants with post-combustion CO_2 capture. It was found that flexibility through CO_2 venting and regenerator under-sizing can significantly increase profitability at low CO_2 prices, but these flexibility measures become uneconomical around a CO_2 price of $40/ton. The very important implication of this finding is that the CO_2 price level where flexibility measures become uneconomical is below the level required for market-driven deployment of CCS technology.

Mac Dowell and Staffell [19] pointed out two important challenges related to post-combustion CCS in future energy systems with high VRE shares. First, the reduced capacity factor and reduced efficiency resulting from the need to balance VRE generators has a large negative effect on levelized costs. Second, the variable production of CO_2 will impose technical and economic difficulties on downstream transport and storage infrastructure. New CCS solutions targeting the power sector must address these important challenges.

1.3. Novel solutions needed for achieving sustainability through VRE

As discussed in the preceding sections, VRE will play a central role in the decarbonization of the global economy, but the need for dispatchable power plants is likely to remain strong. Given the requirement for net-negative emissions later this century, it is a critical sustainable development priority that these dispatchable plants are decarbonized. However, applying CCS to intermittent power generation for balancing VRE poses serious techno-economic challenges, mainly from capital under-utilization and technical challenges related to intermittent CO_2 transport and storage.

The development of novel CCS concepts especially for cost-effective integration of VRE is still a relatively unexplored field of research. One area where work has recently started in this respect is calcium looping applied to coal power plants where cryogenic O_2 storage [20] or regenerated sorbent storage [21] are used for cost-effective flexibility. In particular, the sorbent storage pathway was shown to significantly reduce the capital cost of a plant operating at a reduced capacity factor because of VRE integration [21]. An important limitation of this type of plant is the practically and economically viable size of sorbent storage hoppers, limiting this plant to daily balancing. VRE variability on weekly or seasonal timescales is therefore not addressable by this type of plant.

The present work presents another promising alternative: the gas switching reforming combined cycle (GSR-CC) plant. GSR-CC is a near-zero emission natural gas-fired CO_2 capture plant that maximizes capital utilization and delivers a steady-state CO_2 stream, even when producing intermittent power to balance VRE. In contrast to the calcium looping option mentioned above, GSR-CC employs clean hydrogen as the energy storage mechanism. Hydrogen can be stored over much longer timescales and can also be employed to decarbonize sectors other than power production (electricity currently accounts for only 19% of final energy consumption globally [2]).

The objective of the study is to quantify the economic advantages of the GSR-CC plant when operating at a reduced capacity factor to balance VRE. This novel solution will be benchmarked against

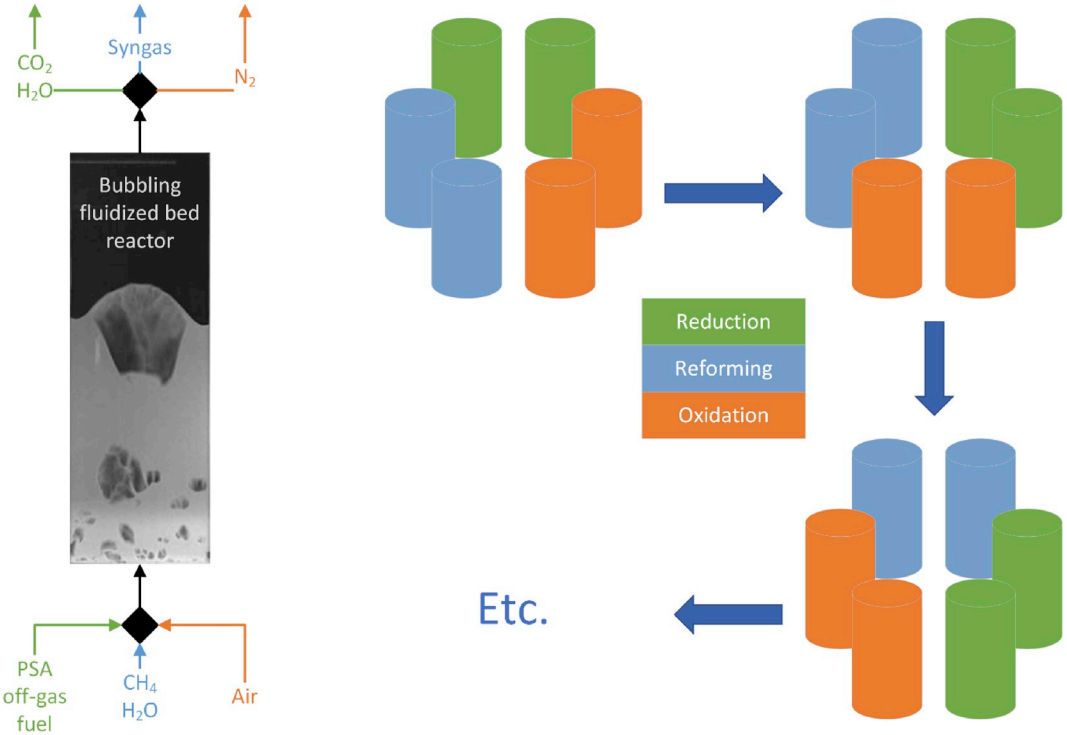

Fig. 2. Left: The gas switching reforming reactor cycles through three steps: reduction, reforming and oxidation. Right: A cluster of gas switching reforming reactors operating as a steady state processing unit.

conventional post-combustion CO_2 capture technology to objectively quantify its potential. This quantitative analysis will be complemented by qualitative discussions of the operational flexibility and risk profile of the GSR-CC plant, followed by recommendations for future work.

2. Gas switching reforming (GSR)

The GSR concept achieves steam methane reforming (SMR) with CO_2 capture at almost no energy penalty. GSR has been experimentally demonstrated at lab scale [22] and assessed for integration with a combined cycle power plant [23] in a configuration called GSR-CC.

GSR is well suited to pure hydrogen production with integrated CO_2 capture due to the synergistic integration with a pressure swing adsorption (PSA) unit [24]. As opposed to the chemical looping reforming [25] technology on which GSR is based, the reduction and reforming steps occur separately so that the remaining carbon-rich fuel gas from the PSA can be combusted with integrated CO_2 capture to provide heat for the endothermic SMR reactions.

As illustrated in Fig. 2, GSR feeds a stream of methane and steam to the reactor in between the reduction and oxidation steps. During this reforming step, the heat from the highly exothermic oxidation step stored in the oxygen carrier material is used to drive the endothermic SMR reactions. Another important requirement is that the oxygen carrier material must be a good SMR catalyst, designating NiO as the most promising candidate.

The GSR-CC concept is well suited to flexible operation because it can produce either electricity or pure hydrogen. Improved process integrations recently proposed [26] maximize this operating flexibility by allowing for almost independent operation of the hydrogen production and power production plants.

The hydrogen production plant, which consists of GSR reactors, water-gas shift (WGS) reactors and a PSA unit, produces a constant stream of pure H_2. When the electricity price is high (low VRE output), this H_2 can be efficiently combusted in the power cycle for profitable power production. When the electricity price is low (high VRE output), it may be more profitable to export the pure H_2 directly instead of combusting it for power production. In this case, the power cycle can be shut down or operated under part-load conditions, with the excess high purity H_2 from the PSA unit being sold directly to the market.

Flexible operation of the GSR-CC plant is therefore dependent on a large market for clean hydrogen. The present study assumes that such markets will develop given the recent resurgence of interest in the hydrogen economy as the scientific and political communities increasingly appreciate its broad applicability and synergies with other energy vectors [27] in addition to its energy security benefits [28].

This ability to operate the H_2 production plant under maximum load throughout its lifetime promises to mitigate the challenge of increasing costs with reduced capacity factors of CCS plants when balancing VRE. In addition, the GSR-CC plant will produce a steady stream of CO_2 even when electricity output varies, thus eliminating the techno-economic concerns of intermittent transport and storage of CO_2.

3. Methods

3.1. GSR process simulation

The schematic of the GSR-CC process for power production is shown in Fig. 3 with stream data given in Table 1. Streams 1, 3 and 4 represent the gas inputs to the reforming, reduction and oxidation steps described in Fig. 2. In the reforming step, natural gas and steam (stream 1) are reformed to syngas (stream 2), which is subsequently fed to a WGS reactor for converting CO to H_2 and a PSA unit for separating high purity H_2.

Off-gases from the PSA unit (stream 3) are compressed, pre-heated and fed back to the GSR reduction stage where all fuel gases are converted to CO_2 and H_2O. This stream is cooled, water is condensed out, and the resulting high purity CO_2 stream is compressed to 110 bar for subsequent transport and storage (stream 7).

Air required for the GSR oxidation step (stream 4) is extracted at the compressor discharge of the gas turbine system of the combined cycle power plant. The N_2-rich stream exiting the oxidation step (stream 6) is fed back to the gas turbine where it could be used to enable a lean premixed combustor for achieving high turbine inlet temperatures with minimal NOx formation [26].

The power plant consists of two gas turbines and two heat recovery steam generators (HRSGs) connected to a single steam turbine system. More details can be found in the description of Case 5 in the aforementioned study [26].

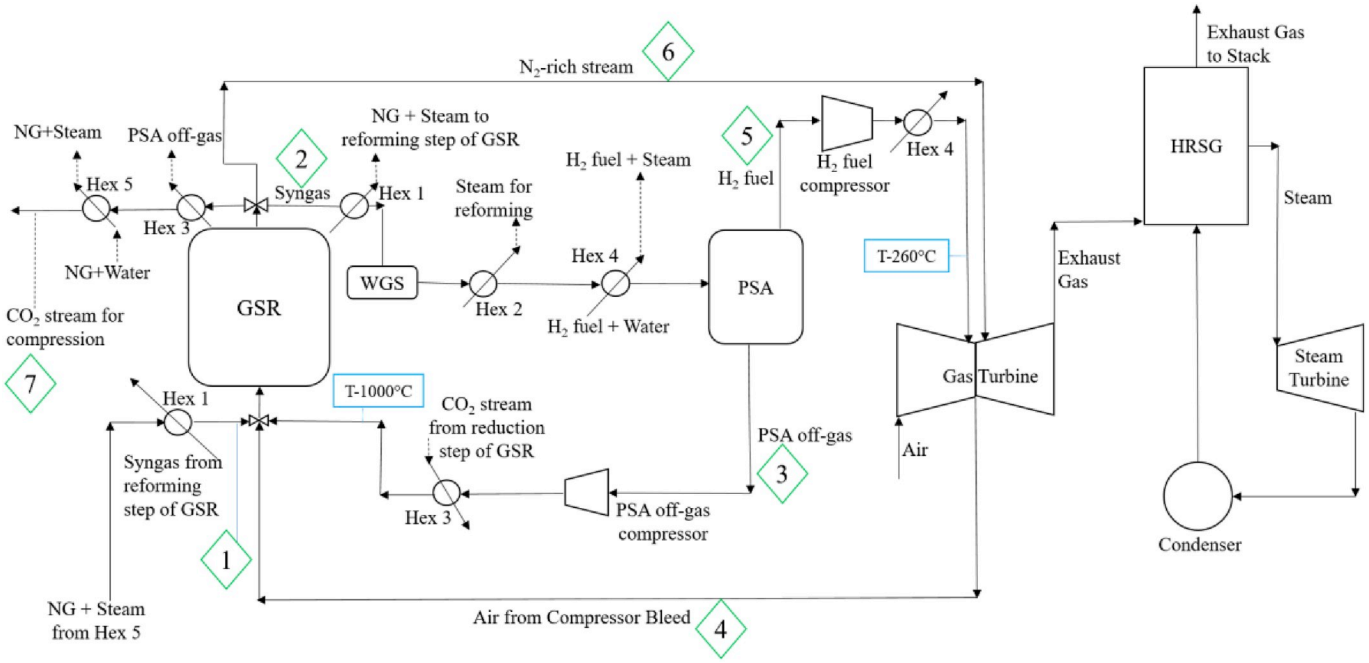

Fig. 3. Schematic of the GSR-CC process in power production mode. Details for the numbered streams are given in Table 1. Modified from Nazir et al. [26].

Table 1
Stream data for the GSR-CC plant in power production mode (Fig. 3).

Stream	P (bar)	T (°C)	Flow (TPH)	H_2O mol%	CO_2 mol%	CH_4 mol%	CO mol%	H_2 mol%	N_2 mol%	O_2 mol%	Ar mol%
1	17.7	895	431	66.7	–	33.3	–	–	–	–	–
2	17.0	1018	447	19.7	3.4	0.7	16.7	59.5	0.1	–	–
3	1.01	25	321	5.0	33.8	2.2	29.4	29.4	0.2	–	–
4	18	417	693	1.0	0.03	–	–	–	77.3	20.74	0.92
5	15	25	46.35	–	–	0.01	–	99.99	–	–	–
6	17	1027	530	3.9	0.8	–	–	0.7	93.4	–	1.1
7	110	25	375	0.3	92.7	–	–	–	6.9	–	0.1

Due to the high purity H_2 produced in the PSA unit, the plant can be operated to export H_2 when the electricity demand is low. This will involve additional unit operations to the GSR-CC process described in Fig. 3, as illustrated by the components coloured red in Fig. 4.

A compressor is needed to feed air to the GSR oxidation step and a gas turbine is required to expand the resulting hot N_2-rich stream. The remaining heat in the N_2 stream is recovered in heat exchanger Hex 7 to prepare saturated 6 bar steam for export. In addition, shifted syngas from the heat exchanger Hex 2 is sent to Hex 6 to produce saturated 6 bar steam for export and cool this stream to the PSA inlet temperature. The H_2 stream from the PSA is compressed in three stages to 150 bar and 30 °C [29], which can be stored or transported.

It is important to minimize the added capital costs involved in operating the plant in H_2 mode rather than electricity mode. For this reason, it will be assumed that the air compression and N_2-stream expansion in H_2 mode can be done in one of the gas turbines already installed for power production, and that Hex 4 in Fig. 3 can serve as Hex 6 in Fig. 4. This equipment sharing between the different plant operating modes could conceivably be achieved with the correct unit sizing and equipment design. To account for inefficiencies with such off-design turbomachinery operation, the economic assessment will assume that no value is derived from the produced 6-bar steam from Hex 6. Hex 7 is neglected in the economic assessment assuming that warm turbine outlet gases are vented to the atmosphere. The added H_2 compressors represent the only unavoidable additional cost involved in building a GSR plant capable of producing H_2 or electricity relative to the GSR-CC plant for electricity production only. This extra compressor cost will therefore be included in the capital cost of the mid-load GSR plant assessed later in this study.

As a simplifying assumption, this work only considers plant performance in full power production mode (Fig. 3) and full H_2 production mode (Fig. 4). Future work will focus on the practicalities of transitioning between these two modes. It is possible that part-load operation proves to be beneficial by allowing the energy extracted in Hex 6 and Hex 7 in Fig. 4 to be used for power production instead of being discarded as currently assumed. Detailed studies on gas turbine operation are also required to investigate the potential of utilizing the hot N_2-rich stream from the GSR oxidation stage to maximize the operating range of the lean premixed combustor.

The complete GSR-CC process except the power plant was modelled

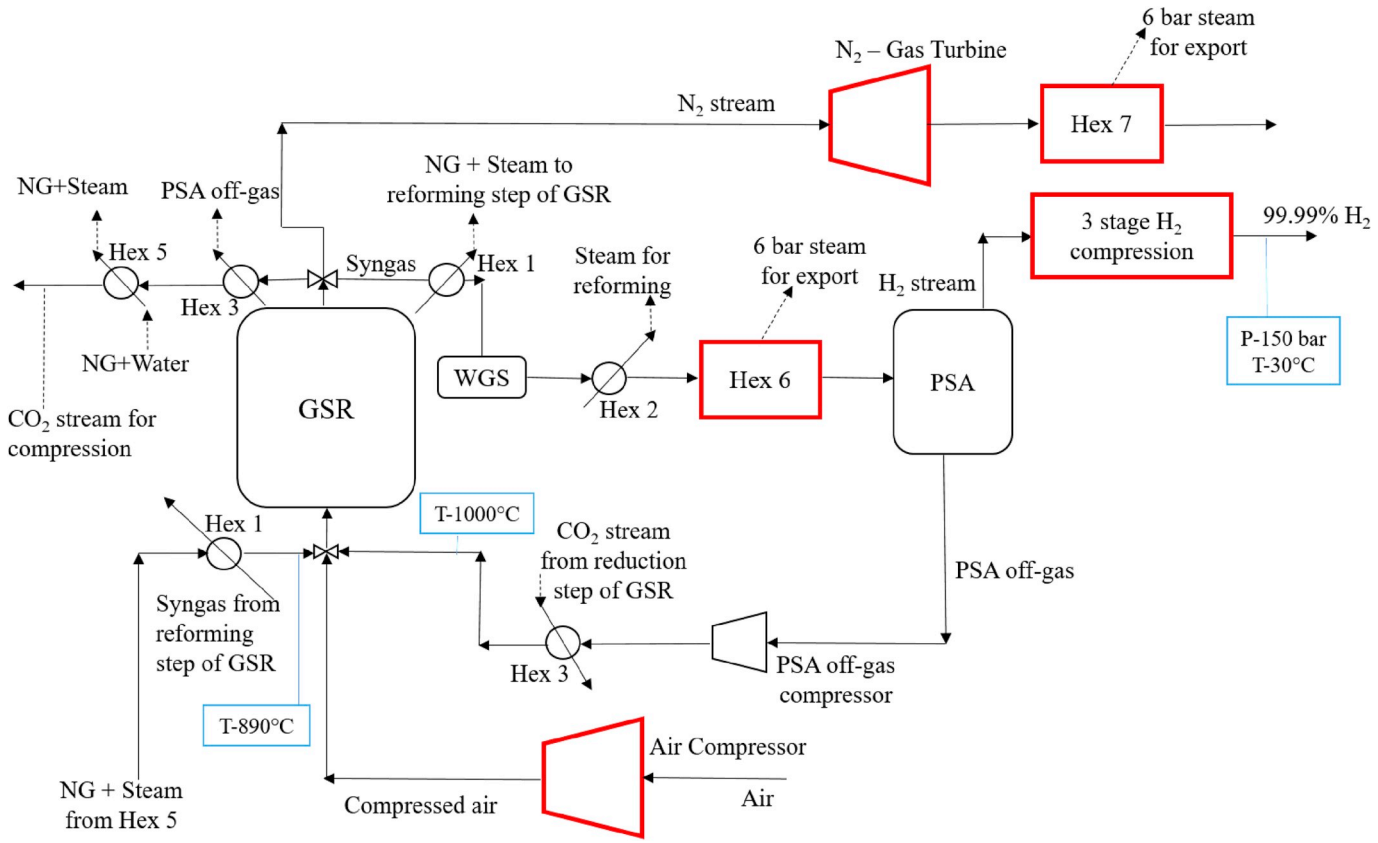

Fig. 4. Schematic of the GSR-CC process in hydrogen production mode. Changes relative to the power production mode (Fig. 3) are indicated in red. (For interpretation of the references to colour in this figure legend, the reader is referred to the Web version of this article.)

in Aspen Hysys V8.6 [30] whereas the power plant was modelled using Thermoflex component of the Thermoflow Suite V26 [31]. The GSR unit was modelled in MATLAB as described in detail in earlier work [23] and the PSA was modelled as a black box according to the performance given in Sircar and Golden [32]. Peng-Robinson equation of state was used to estimate the thermodynamic properties. Additional model parameters are listed in Table 2.

For the GSR-CC process in power production mode, the main technical performance indicators are the net electrical efficiency (Eq. (1)), CO_2 capture ratio (Eq. (2)) and CO_2 avoidance (Eq. (3)). For the GSR plant in hydrogen production mode, the main technical performance indicators are hydrogen production efficiency (Eq. (4)) and its equivalent (Eq. (5)) that also accounts for heat (Q_{th}) and electricity (W_{el}) exports. CO_2 avoidance during H_2 production is calculated according to Eq. (6) by also accounting for the emissions associated with heat and electricity imports [29].

$$\eta = \frac{100\% \times Net\ electricity\ produced\ from\ the\ overall\ process}{LHVofNG\ input\ tothe\ process} \quad (1)$$

$$CCR = \frac{100\% \times CO_2\ captured\ in\ the\ process}{Total\ CO_2\ produced\ in\ the\ process} \quad (2)$$

$$CA = \frac{100\% \times (CO_2\ emitted\ in\ NGCC - CO_2\ emitted\ in\ GSR - CC)}{CO_2\ emitted\ in\ NGCC} \quad (3)$$

$$\eta_{H_2} = \frac{100\% \times \dot{m}_{H2} \times LHV_{H_2}}{\dot{m}_{NG} \times LHV_{NG}} \quad (4)$$

$$\eta_{H_2,eq} = \frac{100\% \times \dot{m}_{H2} \times LHV_{H_2}}{\dot{m}_{NG} \times LHV_{NG} - \frac{Q_{th}}{0.9} - \frac{W_{el}}{0.583}} \quad (5)$$

$$CA_{H_2} = \frac{100\% \times mass\ of\ CO_2\ captured}{\dot{m}_{NG} \times LHV_{NG} \times E_{NG} - Q_{th} \times E_{th} - W_{el} \times E_{el}} \quad (6)$$

In the above equations, E_{NG} is the specific CO_2 emissions per unit of energy input of NG (54.8 g of CO_2 per MJ_{LHV} of NG). Q_{th} is the amount of thermal energy in the 6 bar steam export and is equal to the enthalpy difference in the saturated steam at 6 bar and saturated liquid water at 6 bar W_{el} is the net electrical work in the process. E_{th} (63.3 g_{CO2}/MJ) and E_{el} (97.7 g_{CO2}/MJ) [29] represent the equivalent specific CO_2 emissions per unit of heat and electricity, respectively.

3.2. Economic assessment

3.2.1. Reactor and heat exchanger design

In order to have the desired fluidization velocity of 0.5 m/s, a total cross-sectional area across all the reactors of 244 m^2 is required to process the total volume flowrate of gas that passes through the GSR unit. According to the correlations of Bi and Grace [33], this fluidization velocity is well within the bubbling fluidization regime when typical Geldart B particles with a diameter of 150 μm are used. Using the cost methodology described below, it was determined that a cluster of 64 reactors having a diameter of 2.2 m and a height if 4.4 m would be the option with the lowest cost for the reforming unit. The NiO oxygen carrier selected for this work is highly reactive and achieved equilibrium conversion even in a laboratory scale reactor [22]. It can therefore be reasonably assumed that the selected reactor height will result in good reactor performance.

The reactors operate at a pressure of 18 bar and a maximum temperature of 1100 °C. To facilitate the high temperature and pressure, the reactor wall structure presented in Fig. 5 was proposed. The layers are as follows (from left to right): a high temperature and corrosion-resistant Ni-alloy on the inside to withstand the abrasion of the fluidized bed, 0.73 m insulation in the middle to minimize the heat loss, and a steel shell on the outside to carry the pressure load. The thickness of the insulating material was calculated using Fourier's law assuming 1100 °C inner and 60 °C outer wall temperatures. The ambient temperature was assumed at 25 °C.

The cost estimation was performed according to the cost functions presented in Turton et al. [34]. The reactor was assumed to be constructed of two process vessels: the inner reactor vessel was assumed to be constructed from an expensive Ni-alloy material that does not carry any of the pressure load, while the outer pressure shell was constructed from standard carbon steel and carried the entire pressure load. The cost of the inner reactor vessel was doubled to account for fluidized bed elements like the gas distributor and inlet for oxygen carrier make-up.

Each reactor has a high temperature valve both at the inlet and the outlet. The cost of these valves was estimated according to Hamers et al. [35]. In addition, the cost of the initial load of oxygen carrier material was added to the capital cost of the reactor. The NiO oxygen carrier cost was assumed to be 12.5€/kg [36]. Each component of the reactor cost was updated to the year 2018 using the CEPCI index and converted to Euros using a conversion factor of 1.2 $/€.

The final installed cost breakdown for the cluster of 64 reactors is shown in Fig. 6. The pressure shell and the reactor vessel are the two most important contributors to the total cost. As mentioned later, a process contingency of 30% is added to this reactor cost estimation in the economic assessment to account for the uncertainties arising from the low level of development of GSR technology.

The same cost estimation methodology [34] was applied for the heat exchangers. A shell-and-tube heat exchanger configuration was selected and an energy balance was used to determine the heat flux transferred between the streams using stream data from Nazir et al. [26]. Film and overall heat transfer coefficients were selected from the literature for the calculation of the required heat transfer area [37].

3.2.2. Capital cost estimation

The cost of other components was evaluated using capital cost correlations found in the literature according to Eq. (7). C_0 and Q_0 are the reference cost and capacity of the unit, and M is an exponent that depends on the equipment type. These values are summarized in Table 3. Each value was adjusted to 2018 costs according to the CEPCI index. An install factor of 1.68 was applied to the costs from Franco et al. [38], as installation costs were not included in the cost correlations. However, costs from Spallina et al. [29] are erected costs that do not require an additional installation factor. The compressor reference cost from Smith [39] was calculated to the maximum allowable size of 10 MW using $C_0 = 0.082$, $Q_0 = 0.25$ *and* $M = 0.46$ and also multiplied by a material factor of 3.4 for high grade stainless steel construction [39], after which further scale-up is assumed to occur modularly ($M = 1$). The 1.68 install factor was also applied to this unit.

$$C = C_0 * \left(\frac{Q}{Q_0}\right)^M \quad (7)$$

Adding all the process component installed costs together yields the bare erected cost (BEC). For the calculation of the total overnight cost, the EBTF guidelines [38] were applied as summarized in Table 4, with two modifications. Firstly, a process contingency was added to less mature units based on the guidelines of Rubin et al. [40]: 30% for the

Table 2
Important model parameters used in the GSR-CC simulation.

Turbine inlet temperature	1433 °C
Steam turbine pressure levels	166/32.7/3.4 bar
Maximum GSR cycle temperature	1100 °C
GSR operating pressure	18 bar
Steam to carbon ratio in reforming	2
PSA H_2 recovery	86%
PSA H_2 purity	99.99%
Heat exchanger pressure drop (gas/liquid)	2%/0.4 bar
Turbine polytropic efficiency	83%
Compressor polytropic efficiency	90%

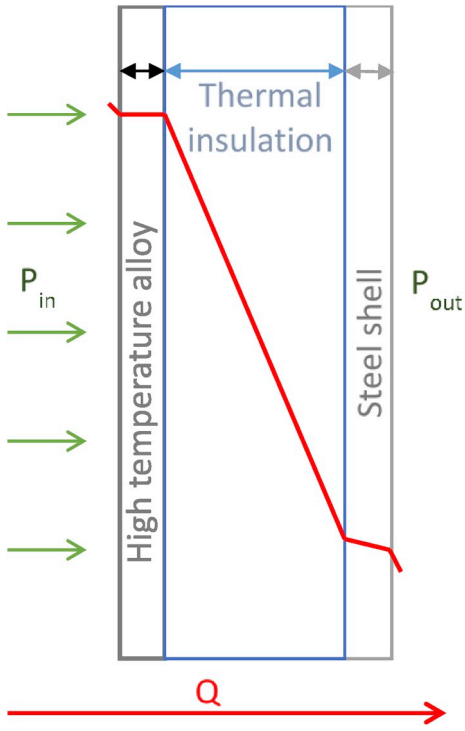

Fig. 5. The reactor wall structure and temperature profile.

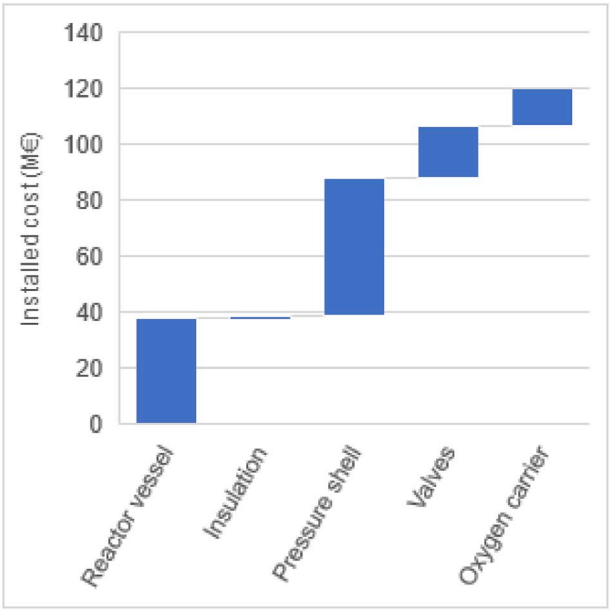

Fig. 6. A cost breakdown for the GSR reactor cluster.

cluster of GSR reactors and the 2-phase flow heat exchangers and 10% for the MEA CO_2 capture system. The rest of the system can be considered mature technologies with a 0% process contingency. Secondly, the owner's cost was increased from 5% used in Franco et al. [38] to 12%, which is an average of this value and three other values (7%, 15% and 22%) listed in Rubin et al. [40].

3.2.3. Operating and maintenance costs

Table 5 presents the assumptions for the fixed and variable operating and maintenance (O&M) costs. The operating labour cost was scaled from the NGCC-MEA plant in Franco et al. [38] proportionately to the output of the plant and was estimated at 12 M€/year. Maintenance and insurance costs were estimated as fraction of the TOC of the plant. The rest of the variable O&M costs were obtained from previous works as indicated in Table 5. A replacement period of 5 years was assumed for the catalyst, oxygen carrier and sorbent. In the case of the MEA replacement costs, both fresh MEA cost and MEA sludge disposal cost was included according to the IEAGHG report [41].

3.2.4. Cash flow analysis

A discounted cash flow analysis was performed to determine the main economic performance indicators of the GSR-CC plant and to compare it with other technologies. Table 6 presents the main assumptions for the analysis for the NGCC-MEA and for the GSR-CC plant. The NGCC plant had the same assumptions, aside from a shorter construction time (2 years).

The levelized cost of electricity (LCOE) was calculated as the electricity price that would yield a net present value (NPV) of zero at the end of the plant's economic lifetime according to Eq. (8). Here, i is the discount rate and ACF is the annual cash flow in every year that consists of capital expenditures linearly distributed over the first three construction years, followed by annual operating income (electricity sales) and expenses (fixed and variable O&M) over a 30-year operating period.

The cost of CO_2 avoidance was calculated according to Eq. (9) using the LCOE [€/MWh] and the CO_2 emissions intensity E [t_{CO2}/MWh]. Here, the subscripts cc and ref indicate the carbon capture and reference NGCC technologies, respectively.

$$NPV = \sum_{t=0}^{n} \frac{ACF_t}{(1+i)^t} \tag{8}$$

$$COCA\left(\frac{€}{tCO_2}\right) = \frac{LCOE_{cc} - LCOE_{ref}}{E_{ref} - E_{cc}} \tag{9}$$

Later, the projected investment return at a fixed electricity and hydrogen price is also calculated. In this case, the annual income of the plant is fixed by these assumed sales prices and the discount rate is adjusted in Eq. (8) to return a zero NPV at the end of the plant lifetime. The discount rate calculated in this manner is representative of the investment return that may be expected under the given assumptions. In the comparative analysis, the plant that returns the highest discount rate using this methodology will be the most attractive option.

4. Results and discussion

4.1. GSR performance

The main results for the technical performance of the GSR-CC process operating to produce power and hydrogen are shown in Table 7. Plant performance in power production mode is identical to Case 5 in Nazir et al. [26]. The net electric efficiency is 51.1% with 98.1% CO_2 avoidance.

In hydrogen production mode, the main power consumption comes from the compression work required to compress PSA off-gas, air, H_2 and CO_2 streams, with the N_2-stream expander cancelling out a little over half of this consumption. Work done by the auxiliaries reduces in hydrogen production mode, since most of the auxiliaries are associated with the power plant section.

The net electrical power of the GSR plant in hydrogen production mode is negative, implying that it will need to import electricity to produce hydrogen, equivalent to 5% of the LHV fuel input. The hydrogen production efficiency and its equivalent for the GSR plant is similar to the conventional steam methane reforming hydrogen plant without CO_2 capture [29], but the GSR plant achieves CO_2 avoidance of 94.1%. CO_2 avoidance is significantly less than CO_2 capture because of emissions associated with imported electricity.

Table 3
Reference costs, capacities and scaling exponents for different process units for use in Eq. (7).

Equipment	Scaling parameter	Reference cost (M€)	Reference capacity	Scaling exponent	Year	Reference
WGS	Thermal input (LHV) [MW]	9.54	1246.06	0.67	2007	[29]
PSA	Inlet flow rate [kmol/hr]	27.96	17069	0.6	2007	[29]
Gas Turbine	Net power output [MW]	49.4	272.12	1	2011	[38]
HRSG	ST gross power [MW]	45.7	292.8	0.67	2011	[38]
Steam Turbine	ST gross power [MW]	33.7	200	0.67	2011	[38]
Steam turbine condenser	ST gross power [MW]	49.8	292.8	0.67	2011	[38]
CO_2 compressor and condenser	Compressor power [MW]	9.95	13	0.67	2011	[38]
MEA CC system	CO_2 captured [kg/s]	28.95	38.4	0.8	2011	[38]
PSA off-gas compressor	Compressor power [MW]	1.52	10	1	2005	[39]
H_2 compressor	Compressor power [HP]	0.0012	1	0.82	1987	[29]

Table 4
The estimation methodology for the total overnight costs of the plant.

Component	Definition
Bare erected cost (BEC)	Install cost of each unit
Process contingency (PS)	0%, 10% or 30% of BEC
Engineering procurement and construction costs (EPCC)	14% of (BEC + PS)
Project contingency (PT)	10% of (BEC + PS + EPCC)
Total plant costs (TPC)	BEC + PS + EPCC + PT
Owners cost (12% of TPC)	12% of TPC
Total overnight costs (TOC)	TPC + Owners costs

Table 5
Fixed and variable operating & maintenance cost assumptions for the GSR plant.

Fixed O&M costs [38]		
Operating labour	12	M€
Maintenance, support and administrative labour	2.5	% of TOC
Property taxes	Included in insurance costs	
Insurance costs	2	% of TOC
Cost of NG	6.5	€/GJ LHV
Process and cooling water [23]		
Process water costs	1.85	€/t
Cooling water make up costs	0.325	€/t
Catalyst and sorbent replacement		
Oxygen carrier	12500 [36]	€/t
WGS catalyst cost	12978 [23]	€/m^3
PSA sorbent replacement costs	907.82 [23]	€/t
MEA replacement cost	(1404.17 + 528.33) [41]	€/t
CO_2 costs [23]		
Transport and storage	10	€/t
Emissions tax	22.68	€/t
Chemicals [42]		
Cooling water chemical treatment	0.0025	€/m^3
Process water chemical treatment	45000	€/mo.

Table 6
Assumptions used in the cash flow analysis.

Economic lifetime	30 years
Discount rate	8%
Construction period	3 years
Capacity factor	85%
First year capacity factor	65%

4.2. Baseload economic assessment

The GSR-CC power plant is compared to two benchmarks: an NGCC power plant with no CO_2 capture and the same NGCC plant with post-combustion MEA CO_2 capture. Table 8 presents the cost breakdown of the three cases.

The LCOE was calculated for each case according to the description around Eq. (8) and the results are presented in Table 9. The two CO_2 capture plants show similar results, with the LCOE in the case of the GSR plant being slightly higher. However, GSR achieved an identical COCA to the MEA plant because of its higher CO_2 avoidance rate.

Fig. 7 shows the breakdown of LCOE for the three different plants. Clearly, fuel costs represent the dominant factor in the levelized costs of

Table 7
The main technical performance indicators of the GSR-CC in power and hydrogen production mode.

Cases	Units	Power mode [26]	Hydrogen mode
Gas Turbine	MW	640.5	–
Steam Turbine	MW	390.6	–
H_2 fuel Compressor	MW	- 5.6	–
PSA off-gas compressor	MW	- 42.6	- 42.6
CO_2 Compressors and Pump	MW	- 18.5	- 18.5
Auxiliaries	MW	- 18.5	- 0.4
Air Compressor	MW	–	- 79.3
N_2-Gas Turbine	MW	–	109.1
3-stage H_2 compression	MW	–	- 60.9
Net electrical power	MW	945.9	- 92.6
Net LHV Input to process	MW	1851	1851
Net Electrical Efficiency (Eq. (1))	% - LHV	51.1	–
CO_2 Capture (Eq. (2))	%	98.7	98.7
CO_2 Avoidance (Eq. (3))	%	98.1	–
Thermal energy in 6 bar steam export (Q_{th})	GJ/hr	–	277.7
Hydrogen production efficiency (Eq. (4))	%	–	83.6
Equivalent hydrogen production efficiency (Eq. (5))	%	–	80.5
H_2 mode CO_2 avoidance (Eq. (6))	%	–	94.1

Table 8
Capital cost breakdown [M€] and performance indicators for the three power plants.

Unit	NGCC	NGCC-MEA	GSR-CC
Heat exchangers			13.8
Gas reformer island			120.0
WGS unit			13.3
PSA			46.8
Gas turbine	159.3	159.3	187.5
HRSG	73.7	72.2	88.4
Steam turbine	69.7	56.6	85.1
Condenser	80.3	93.0	97.4
CO_2 compressor and condenser		23.2	21.8
H_2 compressor			5.2
PSA-off gas compressor			13.1
MEA CO_2 separation system		91.4	
Bare erected cost	382.9	495.8	692.3
Total overnight cost	532.6	702.25	1014.1
Specific total overnight cost [€/kWe]	641.7	989.2	1071.7
Net power production [MW]	829.9	709.9	946.3
Net electric efficiency [%-LHV]	58.3	49.9	51.1
CO_2 avoidance [%]	–	89.7	98.1

Table 9
LCOE and COCA indicators for the three different power plants.

	NGCC	NGCC-MEA	GSR-CC
LCOE [€/MWh]	53.95	73.18	74.95
COCA [€/ton]		60.86	60.86

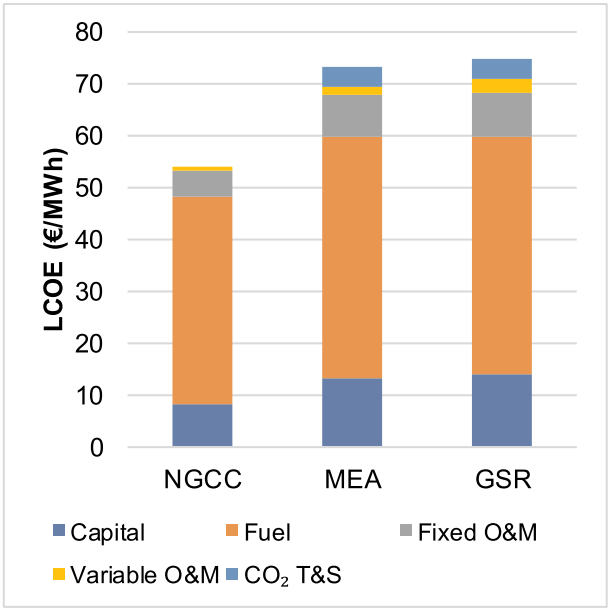

Fig. 7. LCOE breakdown between different cost components for each plant.

all three plants. Capital costs and fixed O&M costs (calculated as a percentage of capital costs) become more influential in the CO_2 capture plants due to their higher specific total overnight costs (Table 8). Relative to the MEA plant, the GSR plant has slightly higher capital costs, which are cancelled out by slightly lower fuel costs. However, GSR also has higher variable O&M costs due to replacement of oxygen carrier material and higher water consumption associated with H_2 production and syngas cooling. CO_2 T&S costs are also significant for the CO_2 capture plants and slightly higher for GSR due to its higher CO_2 capture rate.

As the fuel cost is the dominant element in the plant economics, its variation has the greatest impact on the LCOE and COCA, as presented in Fig. 8. Variation in the plant capacity factor has the second largest impact on the LCOE, with the other three variables having a similar impact.

Finally, Fig. 9 shows the sensitivity of the LCOE of the three power plants to variations in the fuel cost. As expected, the gap between the LCOE of the CO_2 capture plants and that of the NGCC reference plant increases with increasing fuel cost due to the energy penalty imposed by these plants. The GSR energy penalty is slightly smaller than the MEA plant, so it experiences a slightly smaller sensitivity to increasing fuel prices.

4.3. Mid-load economic assessment

The baseload economic assessment presented in the previous section is common practice when assessing different CO_2 capture technologies. However, given the relatively high fuel cost, increasing CO_2 taxes and growth of VRE, it is unlikely that new natural gas-fired power plants will operate under baseload conditions. This section will therefore evaluate the economic performance of the three plants under more realistic mid-load conditions, where most power is produced during times of high system load and/or low VRE power output.

As illustrated earlier in Fig. 1, German mid-load plants (based on hard coal and natural gas) already earn about 22% more than the system average electricity price for the average unit of electricity sold (and about 50% more than the average unit of wind electricity sold). This is the result of these plants generating most of the power during times of high residual demand, leading to high prices. As the growth of VRE continues, these price premiums enjoyed by mid-load plants will probably continue to grow.

For this reason, the results in this section will be expressed as a function of the price premium enjoyed by mid-load plants. In practice, this price premium will primarily depend on the electricity price volatility (influenced by VRE market share) and the plant capacity factor (lower plant utilization results in higher average price premiums as plant output is increasingly concentrated in times of high electricity prices). In this study, the capacity factor will be kept constant at 45% and the price premium will be varied over the range shown in Table 10 to investigate this uncertainty.

Another important simplifying assumption in Table 10 is that the costs and revenues associated with load-following operation are ignored. Power plant efficiency reduces during part-load operation, while start-up and shut-down also imposes additional costs. On the other hand, power plants can earn additional revenues by providing ancillary services by adjusting their power output to balance the grid. In this study, it is assumed that these added costs and added revenues largely cancel out and can therefore be ignored.

It should also be mentioned that the average wholesale power price assumed is higher than the current price in Europe. As recently discussed in the IEA World Energy Outlook [2], current wholesale prices are insufficient to cover the full levelized costs of new power plants. This is primarily due to the subsidized deployment of VRE with near-zero marginal cost and stagnant electricity demand growth. In the future, further VRE expansion will exert downwards pressure on wholesale prices, while increased CO_2 taxes will exert upwards pressure. This study assumes a wholesale price level where moderate returns on investment are possible so that new dispatchable plants can be constructed when needed without additional revenue streams (such as capacity payments).

For GSR, it is assumed that the plant operates in H_2 production mode during times when no electricity is produced to result in a combined capacity factor of 90% over the whole operating year. The added costs of H_2 compressors for allowing H_2 export amounted to €47.2/kWe, thus increasing the plant total overnight cost and fixed O&M cost by 4.5%.

The hydrogen price specified in Table 10 was selected so that it becomes economical for the GSR-CC plant to produce electricity rather than hydrogen when the wholesale electricity price rises above the average market price of €60/MWh. The selected H_2 price is competitive even with current CO_2-intensive hydrogen production through thermochemical fossil fuel conversion and much lower than other clean hydrogen production technologies [43]. This can therefore be viewed as a conservative assumption with substantial upside potential for GSR economic performance.

In addition, it is assumed that the electricity consumption of the GSR plant in H_2 production mode enjoys a discount identical to the price premium during electricity production. This assumption is made because the plant will be producing electricity during times of high electricity prices and hydrogen during times of low electricity prices. As shown in Fig. 10, electricity market data indicates that electricity prices adopt an almost perfect normal distribution, supporting the assumption of an identical discount during hydrogen production to the premium during electricity production.

Finally, it was assumed that the CO_2 transport and storage (T&S) cost for the MEA mid-load plant increases from €10/ton to €15/ton because of the reduced utilization of the T&S infrastructure. This is done under the assumption that T&S costs are distributed evenly between fixed and variable costs. The GSR plant still uses the T&S

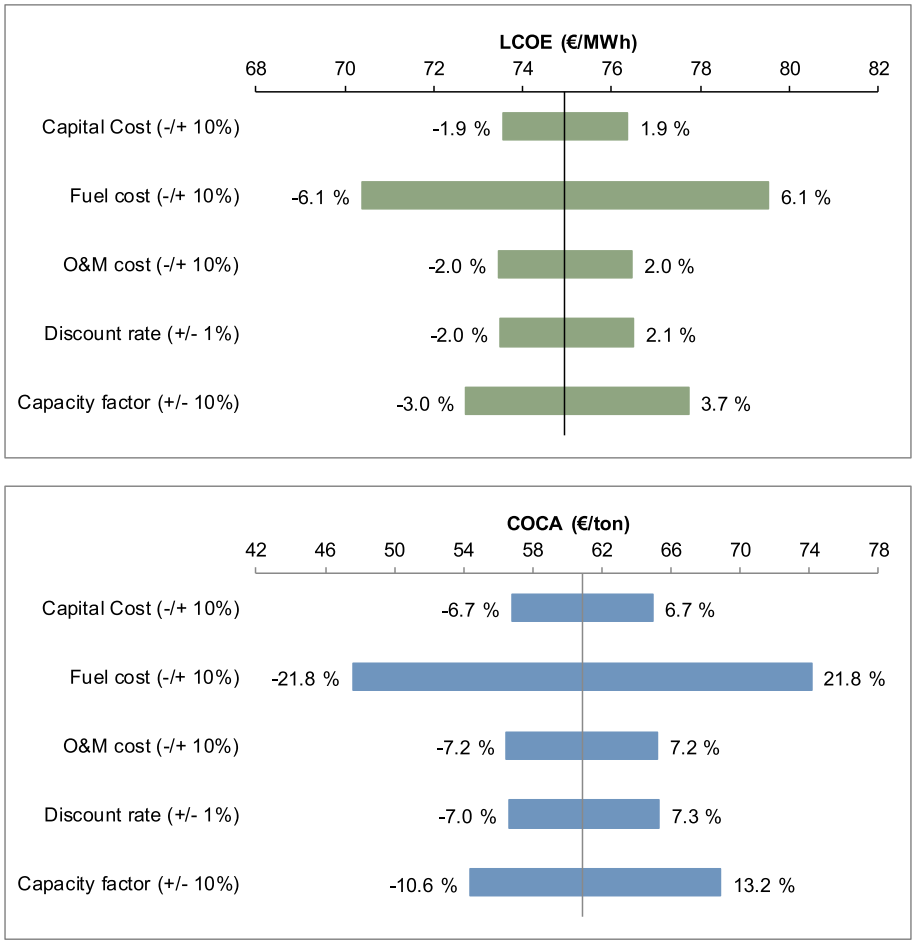

Fig. 8. Sensitivity analysis for the GSR-CC plant. The percentage deviation from the base case is also indicated as data labels for each case.

Fig. 9. Sensitivity of the LCOE of the three different plants to variations in the natural gas price.

infrastructure at maximum capacity, so T&S costs remain at €10/ton.

Using the assumptions in Table 10, the cash flow analysis was repeated for all three plants to calculate the discount rate that returns zero net present value at the end of the plant's economic lifetime. This discount rate is a reasonable approximation of the return that can be expected from the plant capital investment. The expected investment return should be attractive relative to alternatives with similar risk profiles to enable investment in new power plant infrastructure.

Table 10
Assumptions employed in the economic assessment of mid-load plants differing from those in Table 6.

System average wholesale price	60 €/MWh
Mid-load price premium	10-40 €/MWh
Hydrogen sales price	€1.35/kg
Electricity purchase discount	10-40 €/MWh
Capacity factor	45%
H_2 capacity factor	45%
First year capacity factor	30%
CO_2 price	20-100 €/ton
CO_2 T&S cost for MEA & GSR	15 & 10 €/ton
Flexible operation costs	Neglected
Ancillary services revenues	Neglected

Fig. 11 shows the results from this discounted cash flow analysis. As expected, a larger price premium causes substantial increases in the expected investment returns from all three plants. Increasing electricity price volatility from further VRE growth is therefore positive for mid-load plants.

When the CO_2 tax is only €30/ton, the unabated NGCC plant still offers the best investment return. However, investment returns drop strongly when the CO_2 tax increases to €100/ton, showing the risk posed by future CO_2 tax increases. It is noted that the points without any data in Fig. 11 indicate that operating expenses rise above operating income, implying that the plant can no longer make money and

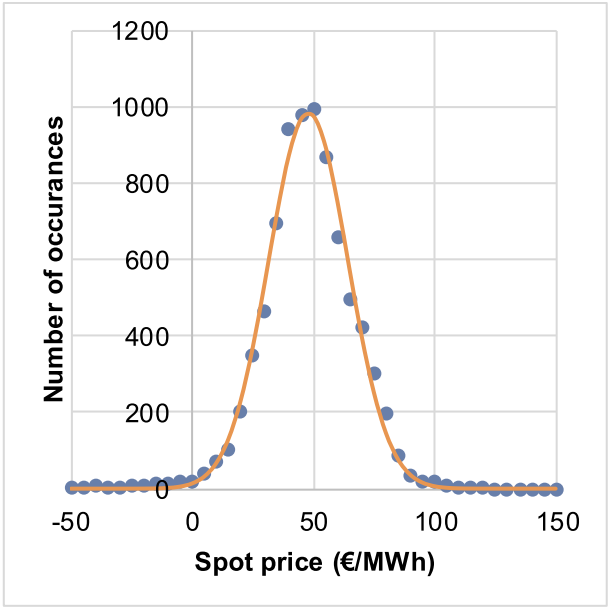

Fig. 10. Distribution of electricity prices over the year 2018 January-November [44]. The data is represented by markers and the line indicates a normal distribution fit to the data.

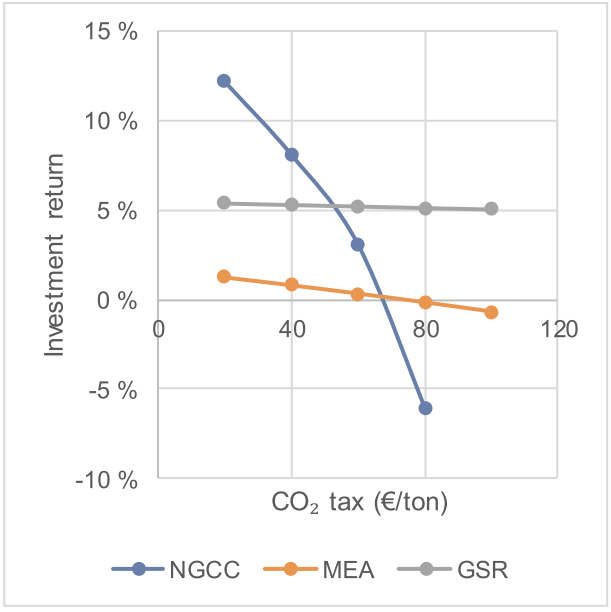

Fig. 12. Annualized return on investment as a function of CO_2 tax at an electricity price premium of €20/MWh.

must be temporarily shuttered or permanently decommissioned. In practice, the plant could also reduce its capacity factor to only produce during times of highest electricity prices, thus increasing the average price premium at the expense of lower electricity sales.

More importantly, the results show that the GSR plant now outperforms the MEA plant, counter to the economic outlook from the baseload economic assessment. Two reasons can be identified: 1) the hydrogen production section is being utilized at 90% capacity factor in GSR, whereas the absorption unit in the MEA plant is only utilized at 45% capacity factor and 2) the MEA plant pays 50% higher CO_2 T&S costs due to the intermittent CO_2 production from this plant.

The economic advantage of the GSR plant over the MEA plant increases with increasing CO_2 price because of the very high CO_2 avoidance of the GSR plant. Fig. 12 demonstrates this trend. It is also shown that the NGCC plant becomes less economically attractive than GSR at a CO_2 tax rate of €53/ton, less economical than the MEA plant at a CO_2 tax rate of €69/ton and must be shuttered at a CO_2 tax above €80/ton.

A breakdown of operating income and expenses for one operating year is shown for all three plants in Fig. 13. The €100/ton CO_2 tax strongly increases the expenses of the NGCC plant, almost to the level of the fuel costs, causing annual expenses to exceed annual income. The costs associated with CO_2 taxes and T&S costs for the MEA and GSR plants are much smaller. Fig. 13 also shows that the cash flows for the GSR plant are much larger due to its high overall capacity factor. Income from electricity sales is substantially larger than hydrogen sales because of the price premium on electricity sales.

Finally, a few qualitative observations about the investment risk profiles of the different plants can be made. As mentioned earlier, the NGCC plant's economic performance is sensitive to large increases in the CO_2 tax. Such tax increases must happen if global temperatures are to be kept below 2 °C [2], but the timeframes within which this dynamic will play out remains highly uncertain.

If the NGCC plant is constructed to be CCS-ready, this risk reduces substantially because a CCS retrofit (potentially with MEA technology)

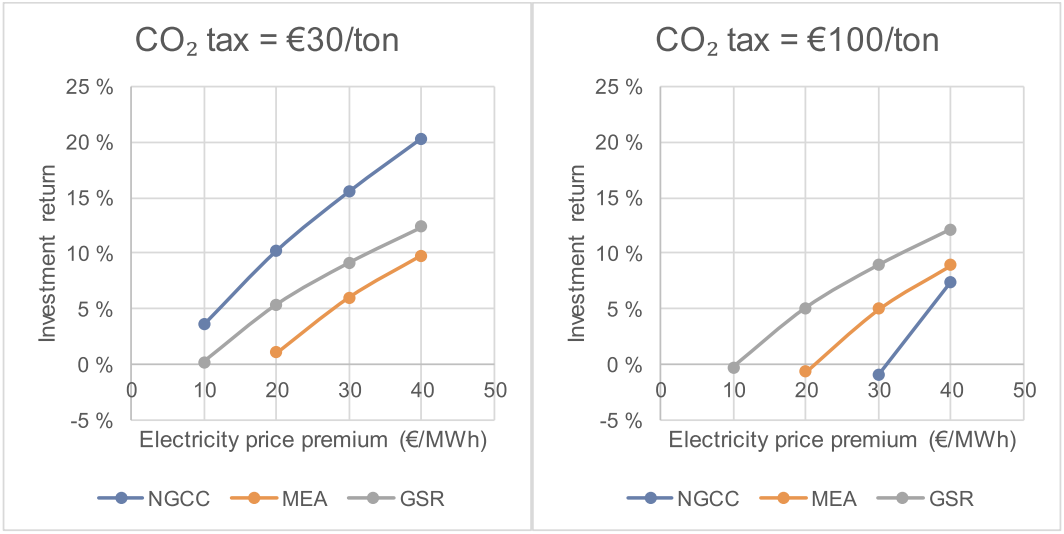

Fig. 11. Annualized return on investment as a function of the electricity price premium received by the mid-load plant at two different CO_2 tax rates.

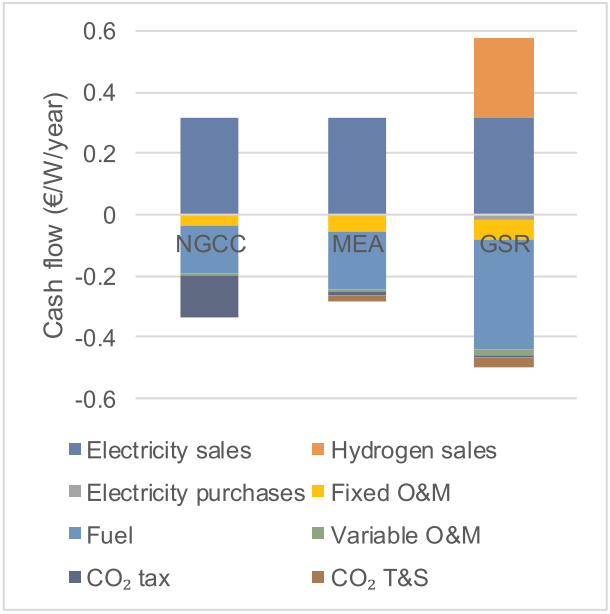

Fig. 13. Breakdown of annual operating cash flow at a CO_2 tax of €100/ton and a price premium of €20/MWh.

can restore profitable operation after large CO_2 tax hikes. However, flexible operation of an NGCC plant with MEA CO_2 capture technology will pose some technical and economic challenges in the capture, transport and storage parts of the CCS value chain. As discussed in the introduction, MEA technology can aid in flexible operation, but the equipment oversizing required for this purpose is unlikely to be economical at CO_2 price levels required for market-driven CCS deployment [18]. In addition, intermittent CO_2 production can create problems for downstream CO_2 T&S [19].

The GSR plant should be just as flexible as an NGCC plant, with a potential to deploy the hot N_2-stream from GSR to further improve startup times and mitigate the minimum environmental load restriction of the gas turbine. In addition, the constant output of CO_2, even under flexible power output will simplify CO_2 T&S.

The primary risk related to GSR is the current lack of a large market for clean hydrogen. As mentioned earlier, the assumed hydrogen price in this study (€1.35/kg) is low compared to other options for clean hydrogen production. GSR will therefore perform well if the hydrogen economy is eventually realized. If CO_2 prices increase according to the requirements for 2 °C global warming and VRE expansion continues, hydrogen appears increasingly attractive as a carbon neutral energy carrier and storage mechanism. A rising sense of urgency about climate change therefore increases the likelihood that this primary requirement for investment in the GSR-CC plant will be fulfilled in the medium-term future.

If a large market for clean hydrogen is established, the ability of the GSR-CC plant to alternate between two valuable products will significantly reduce investment risk. The plant will be able to capitalize on profitable opportunities presented by price spikes in either electricity or hydrogen and will only be under economic pressure if prices for both commodities crash simultaneously. In addition, the very high CO_2 avoidance of the GSR plant makes it insensitive to CO_2 tax increases.

Given all these considerations, investment in the GSR-CC plant appears highly attractive if a large clean hydrogen market is established, which, in turn, appears likely upon a meaningful commitment to keeping global warming below 2 °C.

5. Summary and conclusions

This study investigated the new gas switching reforming combined cycle (GSR-CC) plant that can flexibly convert natural gas to electricity (during low VRE output) or hydrogen (during high VRE output) with near-zero CO_2 emissions. In this way, this novel energy conversion plant overcomes the two most important techno-economic challenges facing flexible CCS: low capital utilization rates and the need for intermittent CO_2 transport and storage. In addition, clean hydrogen produced during times of high VRE output can aid in the decarbonization of sectors other than electricity.

A standard baseload economic assessment at a capacity factor of 85% revealed that the GSR combined cycle power plant has a slightly higher LCOE than the benchmark NGCC plant with MEA post-combustion CO_2 capture (74.95 €/MWh for GSR and 73.18 €/MWh for MEA). However, a more realistic mid-load scenario at a capacity factor of 45% reversed this outcome. When assuming an average electricity price of €60/MWh and a €1.35/kg hydrogen price, the GSR plant outperformed the MEA benchmark, showing an annualized investment return that is about 5 %-points higher. This advantage increased with higher CO_2 prices due to the very high CO_2 avoidance of the GSR plant.

The significant improvement in the GSR economic performance under mid-load operation is due to its high utilization of the CO_2 capture, compression, transport and storage equipment relative to the MEA benchmark. This feature of the GSR plant not only brings large economic benefits, but will also address the technical challenges related to intermittent influxes of CO_2 into a large future CO_2 transport and storage network. Given the rising importance of VRE in global decarbonization efforts, the development of CO_2 capture plants with these characteristics must be given high priority.

The primary requirement for the feasibility of the GSR plant is the establishment of a large market for clean hydrogen. Once such a market is established, the GSR plant will have an attractive risk profile relative to other CCS power plants, with reduced exposure to fluctuating electricity prices and the ability to avoid the techno-economic challenges related to intermittent CO_2 supply to downstream transport and storage infrastructure. This good economic performance and risk reduction merits further research into the GSR combined hydrogen and power plant.

Two key subjects are recommended for future work. First, the flexible operation of the GSR-CC plant must be studied in detail, including thermodynamic performance under part-load operation and detailed assessments of the load flexibility of the lean pre-mixed H_2 combustor. Second, power system simulations aiming to quantify the impact of the GSR-CC plant on total system costs in an environment with high VRE market share and CO_2 prices are strongly recommended.

Declarations of interest

None.

Acknowledgement

The current work is part of “GaSTech” project under the Horizon 2020 programme, ACT Grant Agreement No. 691712. The authors gratefully acknowledge the funding authorities: Romanian National Authority for Scientific Research and Innovation (CCCDI – UEFISCDI), Research Council of Norway and the European Commission.

References

[1] IPCC. Global warming of 1.5 °C. Intergovernmental Panel on Climate Change; 2018.
[2] IEA. World energy outlook. International Energy Agency; 2018.
[3] IEA. Tracking clean energy progress. International Energy Agency; 2018https://www.iea.org/tcep/, Accessed date: 18 December 2018.
[4] IPCC. Fifth assessment report: mitigation of climate change. Intergovernmental panel on Climate Change; 2014.
[5] IRENA. Renewable power generation costs in 2017. International Renewable Energy Agency; 2018.
[6] Hirth L. The market value of variable renewables: the effect of solar wind power variability on their relative price. Energy Econ 2013;38:218–36.

[7] Burger B. Power generation in Germany - assessment of 2017. 2018https://www.ise.fraunhofer.de/content/dam/ise/en/documents/publications/studies/Stromerzeugung_2017_e.pdf, Accessed date: 18 December 2018.
[8] Hirth L. Market value of solar power: is photovoltaics cost-competitive? IET Renew Power Gener 2015;9:37–45.
[9] McKinsey. Energiewende-index. 2018https://www.mckinsey.de/branchen/chemie-energie-rohstoffe/energiewende-index#umweltschutz, Accessed date: 18 December 2018.
[10] Hirth L, Ueckerdt F, Edenhofer O. Integration costs revisited – an economic framework for wind and solar variability. Renew Energy 2015;74:925–39.
[11] Jacobson MZ, Delucchi MA. Providing all global energy with wind, water, and solar power, Part I: technologies, energy resources, quantities and areas of infrastructure, and materials. Energy Policy 2011;39:1154–69.
[12] Clack CTM, Qvist SA, Apt J, Bazilian M, Brandt AR, Caldeira K, et al. Evaluation of a proposal for reliable low-cost grid power with 100% wind, water, and solar. Proc Natl Acad Sci 2017;114:6722.
[13] Hirth L, Steckel JC. The role of capital costs in decarbonizing the electricity sector. Environ Res Lett 2016;11:114010.
[14] Donovan C, Corbishley C. The cost of capital and how it affects climate change mitigation investment. Grantham Institute Briefing 2016. paper No 15.
[15] Brouwer AS, van den Broek M, Zappa W, Turkenburg WC, Faaij A. Least-cost options for integrating intermittent renewables in low-carbon power systems. Appl Energy 2016;161:48–74.
[16] Brouwer AS, van den Broek M, Seebregts A, Faaij A. Operational flexibility and economics of power plants in future low-carbon power systems. Appl Energy 2015;156:107–28.
[17] van der Wijk PC, Brouwer AS, van den Broek M, Slot T, Stienstra G, van der Veen W, et al. Benefits of coal-fired power generation with flexible CCS in a future northwest European power system with large scale wind power. Int J Greenh Gas Control 2014;28:216–33.
[18] Oates DL, Versteeg P, Hittinger E, Jaramillo P. Profitability of CCS with flue gas bypass and solvent storage. Int J Greenh Gas Control 2014;27:279–88.
[19] Mac Dowell N, Staffell I. The role of flexible CCS in the UK's future energy system. Int J Greenh Gas Control 2016;48:327–44.
[20] Zhou L, Duan L, Anthony EJ. A calcium looping process for simultaneous CO2 capture and peak shaving in a coal-fired power plant. Appl Energy 2019;235:480–6.
[21] Astolfi M, De Lena E, Romano MC. Improved flexibility and economics of Calcium Looping power plants by thermochemical energy storage. Int J Greenh Gas Control 2019;83:140–55.
[22] Wassie SA, Gallucci F, Zaabout A, Cloete S, Amini S, van Sint Annaland M. Hydrogen production with integrated CO2 capture in a novel gas switching reforming reactor: proof-of-concept. Int J Hydrogen Energy 2017;42:14367–79.
[23] Nazir SM, Cloete S, Bolland O, Amini S. Techno-economic assessment of the novel gas switching reforming (GSR) concept for gas-fired power production with integrated CO2 capture. Int J Hydrogen Energy 2018;43:8754–69.
[24] Francisco Morgado J, Cloete S, Morud J, Gurker T, Amini S. Modelling study of two chemical looping reforming reactor configurations: looping vs. switching. Powder Technol 2017;316:599–613.
[25] Rydén M, Lyngfelt A, Mattisson T. Synthesis gas generation by chemical-looping reforming in a continuously operating laboratory reactor. Fuel 2006;85:1631–41.
[26] Nazir SM, Cloete JH, Cloete S, Amini S. Gas switching reforming (GSR) for power generation with CO2 capture: process efficiency improvement studies. Energy 2019;167:757–65.
[27] Moliner R, Lázaro MJ, Suelves I. Analysis of the strategies for bridging the gap towards the Hydrogen Economy. Int J Hydrogen Energy 2016;41:19500–8.
[28] Demirbas A. Future hydrogen economy and policy. Energy Sources B Energy Econ Plan Policy 2017;12:172–81.
[29] Spallina V, Pandolfo D, Battistella A, Romano MC, Van Sint Annaland M, Gallucci F. Techno-economic assessment of membrane assisted fluidized bed reactors for pure H2 production with CO2 capture. Energy Convers Manag 2016;120:257–73.
[30] AspenHYSYS. Aspen HYSYS V8.6 user guide. Bedford, Massachusetts, USA: Aspen Technology Inc.; 2017.
[31] Thermoflow. Thermoflow suite V26 user guide. Southborough, MA, USA: Thermoflow Inc.; 2017.
[32] Sircar S, Golden TC. Purification of hydrogen by pressure swing adsorption. Separ Sci Technol 2000;35:667–87.
[33] Bi HT, Grace JR. Flow regime diagrams for gas-solid fluidization and upward transport. Int J Multiph Flow 1995;21:1229–36.
[34] Turton R, Bailie RC, Whiting WB, Shaeiwitz JA. Analysis, synthesis and design of chemical processes. Pearson Education; 2008.
[35] Hamers HP, Romano MC, Spallina V, Chiesa P, Gallucci F, MvS Annaland. Comparison on process efficiency for CLC of syngas operated in packed bed and fluidized bed reactors. Int J Greenh Gas Control 2014;28:65–78.
[36] Adanez J, Abad A, Garcia-Labiano F, Gayan P, de Diego LF. Progress in chemical-looping combustion and reforming technologies. Prog Energy Combust Sci 2012;38:215–82.
[37] Bergman TL, Lavine AS, Incropera FP, Dewitt DP. Fundamentals of heat and mass transfer. seventh ed. John Wiley and Sons; 2011.
[38] Franco F, Anantharaman R, Bolland O, Booth N, van Dorst E, Ekstrom C, et al. European best practice guidelines for CO2 capture technologies. CESAR project: European Seventh Framework Programme; 2011.
[39] Smith R. Chemical process: design and integration. Wiley; 2005.
[40] Rubin E, Booras G, Davison J, Ekstrom C, Matuszewski M, McCoy S, et al. Toward a common method of cost estimation for CO2 capture and storage at fossil fuel power plants. Global CCS institute; 2013.
[41] Hooey L, Boden A, Larsson M, Knights M, Johns J, Abraham V, et al. Iron and steel CCS study (techno-economics integrated steel mill). International Energy Agency (IEAGHG); 2013.
[42] Cormos A-M, Cormos C-C. Techno-economic evaluations of post-combustion CO2 capture from sub- and super-critical circulated fluidised bed combustion (CFBC) power plants. Appl Therm Eng 2017;127:106–15.
[43] Nikolaidis P, Poullikkas A. A comparative overview of hydrogen production processes. Renew Sustain Energy Rev 2017;67:597–611.
[44] EXAA. HIstorical spot market data. Energy Exchange Austria; 2018.